A Comparison of VLC Receivers That Incorporate Two Different SiPMs

Zubair Ahmed, Wajahat Ali, Grahame Faulkner, and Steve Collins

***Abstract*—Previously, when selecting silicon photomultipliers (SiPMs) for use in visible light communications (VLC) systems the bandwidth of the SiPM has been a high priority. However, results of experiments on VLC receivers containing two different sizes of commercially available SiPMs show that, if equalization is used and the OOK bit time is less than one third of the duration of its output pulses, the SiPMs bandwidth doesn't significantly impact the receiver's performance. Consequently, for these data rates the criteria used to select which SiPM to incorporate in VLC receivers should put a higher priority on their area and photon detection efficiency than on their bandwidth. In addition, for these data rates, unless the SiPM becomes non-linear, the performance of a receiver containing a SiPM can be predicted based upon Poisson statistics.**

***Index Terms*—Optical wireless communications, silicon photomultiplier, visible light communications.**

I. Introduction

THE Shannon-Hartley theorem suggests that the maximum data rate of any communications systems depends upon its bandwidth and signal to noise ratio (SNR). Consequently, the best possible receivers for visible light communications (VLC) [1] have a relatively wide bandwidth and best possible SNR [2]. It is this last characteristic of an ideal receiver which has motivated research into using silicon photomultipliers (SiPMs) in VLC receivers [3], [4], [5], [6], [7], [8], [9], [10], [11], [12], [13], [14], [15], [16], [17], [18], [19], [20], [21], [22], [23].

SiPMs produced by Broadcom, Hammamatsu and onsemi$_{\mathrm{TM}}$ are arrays of microcells that each contain an avalanche photodiode (APD) in series with a resistor. However, the available SiPMs have different characteristics, including their areas, photon detection efficiencies, number of microcells and output pulse widths. This variety of SiPMs and the difficulty performing RF experiments carefully means that a comprehensive experimental comparison of the performance of receivers containing all the different SiPMs would be time consuming. However, the Shannon-Hartley theorem suggests that the bandwidth of a VLC system is more important than its SNR. Consequently, SiPMs with fast output pulses, and therefore wide bandwidths, have been incorporated into most experimental VLC systems [17], [18], [19], [21], [22], [23].

Many VLC systems are free space systems, and hence an important characteristic of a receiver is the irradiance at the receiver needed to achieve the required combination of data rate and bit error rate (BER) [22]. The Poisson statistics of the dominant noise source in a SiPM means that the BER is determined by the number of detected photons in a bit time. Consequently, the irradiance required to achieve a required BER and OOK data rate can be reduced by increasing the area of a SiPM. Unfortunately, the larger available SiPMs have wider output pulses and therefore a smaller bandwidth.

In this paper the results of a comparison of the performance of VLC receivers containing two different sizes of SiPM are reported. The larger SiPM has four times the area of the smaller SiPM but half its bandwidth. These characteristics and the Shannon-Hartley theorem mean that the receiver containing the smaller SiPM is expected to perform better than the receiver containing the larger SiPM. However, a comparison of results obtained with receivers containing the two SiPMs shows that this is not always the case. In particular, the comparison shows for the first time that, if equalization is used and the OOK bit time is less than one third of the duration of the SiPM's output pulses, the bandwidth of the SiPM doesn't affect the performance of the receiver. In addition, results are presented which show that, until the SiPM's response becomes non-linear, the performance of SiPM receivers for these data rates can be predicted accurately using Poisson statistics alone. In the future it will therefore be possible to compare the performance of receivers containing a wide variety of different SiPMs in a variety of scenarios without the need for time consuming experiments.

The paper is organized as follows. Poisson statistics are used to predict the expected relative performance of SiPMs with different area in Section II. However, this prediction doesn't take into account the non-linear response of SiPMs and the smaller bandwidth of the larger SiPM, which are investigated in Sections III and IV respectively. Section V then contains a description of results from data transmission experiments with receivers containing the two different SiPMs before and after decision feedback equalization (DFE) has been applied. In Section VI results are presented which show that, once DFE

Manuscript received 26 September 2022; revised 27 November 2022; accepted 18 January 2023. Date of publication 23 January 2023; date of current version 7 April 2023. This work was supported in part by the Punjab Educational Endowment Fund - Pakistan, and in part by the U.K. Engineering and Physical Sciences Research Council (EPSRC) under Grant EP/R00689X/1. *(Corresponding author: Steve Collins.)*

Grahame Faulkner and Steve Collins are with the Department of Engineering Science, University of Oxford, OX1 2JD Oxford, U.K. (e-mail: grahame.faulkner@eng.ox.ac.uk; steve.collins@eng.ox.ac.uk).

Zubair Ahmed is with the Department of Engineering Science, University of Oxford, OX1 2JD Oxford, U.K., and also with the School of Engineering and Physical Sciences, Heriot-Watt University, EH14 4AS Edinburgh, U.K. (e-mail: z.ahmed@hw.ac.uk).

Wajahat Ali is with the Department of Engineering Science, University of Oxford, OX1 2JD Oxford, U.K., and also with the Department of Engineering, University of Cambridge, CB2 1TN Cambridge, U.K. (e-mail: wa279@cam.ac.uk).

Digital Object Identifier 10.1109/JPHOT.2023.3239112

TABLE I
KEY PARAMETERS AND THEIR VALUES OF TWO J-SERIES SIPMS OBTAINED FROM THE MANUFACTURES DATASHEET [24]

Parameter	30035	60035
Area [mm^2]	9.42	36.84
Maximum Breakdown Voltage [V]	24.7	24.7
Number of Microcells	5675	22292
Microcell size [µm]	35	35
Fill factor [%]	75	75
Recovery Time [ns]	45	50
PDE [405 nm]	0.5 (@ 6V)	0.5 (@ 6V)
Dark Count Rate [MHz]	1.3 (@ 6V)	5.2 (@ 6V)
Pulse width of fast output [ns]	1.5	3.0

has been applied, Poisson statistics can be used to predict the performance of a VLC system that includes a receiver containing a SiPM operating in its linear regime for all OOK data rates whose bit time is less than one third of the SiPMs output pulse width. However, in some cases an accurate prediction is only achieved if variations between the fast output pulses are taken into account. Finally, Section VII contains concluding remarks.

II. RELATIVE PERFORMANCE OF TWO SIPMS

All the microcells in SiPMs are biased in parallel so that the voltage across all the APDs is above their breakdown voltage. This means that a photon can create an avalanche process. Without the resistor this avalanche would be self-sustaining. However, an avalanche event causes a voltage drop across the resistor which reduces the voltage across the APD so that the avalanche process is quenched. After it has been quenched the microcell has to be recharged. Unfortunately, during this recovery process the bias voltage on the microcell is less than its maximum. Consequently, the microcell isn't as effective at detecting photons. If a single microcell is used as a receiver the recovery time would limit the achievable data rate. This limitation is avoided by using SiPMs that contain thousands of microcells. So that photons can be detected the SiPMs manufactured by onsemi$_{\mathrm{TM}}$ have a fast output created by capacitively coupling the voltage change across each APD to a shared output line. The wider bandwidth created by the narrower pulses on the fast output means that SiPMs manufactured by onsemi$_{\mathrm{TM}}$ have previously been incorporated in VLC receivers [17], [18], [19], [21], [22], [23].

Table I contains the important characteristics of two SiPMs manufactured by onsemi$_{\mathrm{TM}}$. Both of these SiPMs contain the same design of microcells and hence the most significant difference between them is that the 60035 is four times larger than the 30035. This increase in area is significant because in many VLC applications the power available at the transmitter will be limited by the need to make an eye-safe system or a desire to limit the power consumption of the transmitter. The divergence of the transmitters output will then determine the irradiance, rather than power, at the receiver. Consequently, an important performance metric for a receiver is the irradiance required to support a data rate with an acceptable BER [22].

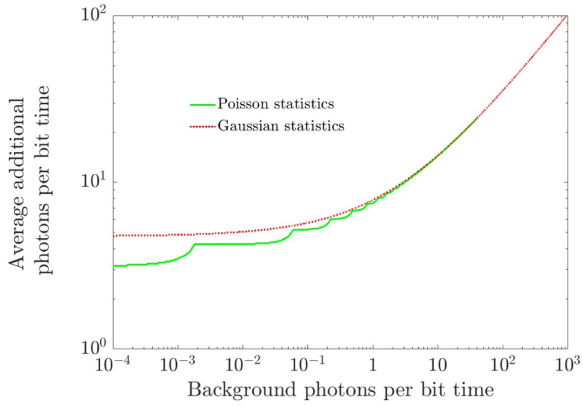

Fig. 1. A comparison of two methods of estimating the average additional photons per bit needed to transmit OOK data as the number of background photons per bit time is varied.

For any photon-counting receiver, including an ideal SiPM, the number of photons detected in a bit time is determined by Poisson statistics. Then the BER can be calculated using

$$BER = \frac{1}{2}\left[\sum_{k=0}^{n_T} \frac{(N_{Tx}+N_b)^k}{k!}.e^{-(N_{Tx}+N_b)} + \sum_{k=n_T}^{\infty} \frac{(N_b)^k}{k!}.e^{-N_b}\right] \quad (1)$$

where N_b is the average number of photons detected per bit time when a zero is received and N_{Tx} is the number of additional photons per bit time from the transmitter when a one is received. The values of N_{Tx} required to achieve a BER of 10^{-3} at different values of N_b, calculated using (1), are shown in Fig. 1. These results show that, for this BER, if N_b is less than 2×10^{-4}, N_{Tx} is independent of N_b. In this regime increasing the area of a SiPM will increase N_b but will not increase N_{Tx} significantly. Under these conditions increasing the SiPM area by a factor M will reduce the irradiance from the transmitter required to achieve the same BER and data rate by a factor of M. Under these conditions we would expect the 30035 to require four times the irradiance required by the 60035 to support the same BER and data rate.

The results in Fig. 1 also show that when N_b is greater than 10 the results obtained assuming Poisson and Gaussian (normal) statistics are indistinguishable. When the noise in a receiver has a Gaussian distribution and OOK data is transmitted the measure of the signal to noise ratio that determines the BER is Q,

$$Q = \frac{V_S^{PP}}{v_{n,0}^{rms} + v_{n,1}^{rms}} \quad (2)$$

where is V_S^{PP} the difference between the mean receiver output signals when the two different bits are received and $v_{n,0}^{rms}$ and $v_{n,1}^{rms}$ are respectively the noise when a zero and a one are being received. All these three quantities are calculated from statistics gathered at times when transmitted bits are decoded. When the Gaussian distributions arise from Poisson statistics the noise in the receiver output will be proportional to the square root of the number of detected photons. Consequently, (2) becomes

$$Q = \frac{N_{Tx}}{\sqrt{N_{Tx} + N_b} + \sqrt{N_b}} \tag{3}$$

However, as shown in Fig. 1, N_{Tx} increases more slowly than N_b and so eventually $N_b > N_{Tx}$ and then (3) becomes

$$Q \approx \frac{N_{Tx}}{2\sqrt{N_b}} \tag{4}$$

In this regime if the area of a SiPM is increased by a factor M the irradiance from the transmitter needed to support the same BER and data rate decreases by a factor of $\sqrt{\text{M}}$. Under these conditions the 30035 is expected to require double the irradiance required by the 60035.

However, these predictions of the relative performance of the 30035 and the 60035 don't take into account two potentially important phenomena. The first of these is the non-linear response of SiPMs. The second is the different widths of the fast output pulses used to detect photons.

III. Non-Linear Response of SiPMs

The non-linear response of a SiPM is a consequence of the need to recharge each microcell after it has been quenched. However, the capacitance of the APD in each microcell and the resistance connecting it to the source of the bias means that this recharging process requires a recovery time, typically lasting several nanoseconds. It is this recovery time which creates a non-linear relationship between the response of a SiPM and the irradiance falling on it. The voltage source used to bias the SiPM has to supply the current needed to recharge each microcell's capacitance. Consequently, the nonlinear response of a SiPM can be observed by measuring the current supplied by this voltage source as the irradiance falling on the SiPM is varied [17], [21].

Fig. 2 shows the measured current required to sustain the bias voltage across a 30035 and a 60035 for varying irradiances from a 405 nm laser diode. Although the 30035 and 60035 contain the same design of microcell the recovery time of the 60035 is slightly longer than the recovery time of the 30035. Consequently, as shown in Fig. 2, the response of the 30035 deviates by 50% from the extrapolated linear response at an irradiance of approximately 1.2 mWm^{-2} and at 0.94 mWm^{-2} for the 60035.

The bit error rate is determined by the number of photons per bit and the 60035 is four times larger than the 30035. Consequently, although, the 60035 exhibits a non-linear response at a slightly lower irradiance than a 30035 the non-linearity is expected to impact the 30035 at significantly lower data rates than the 60035.

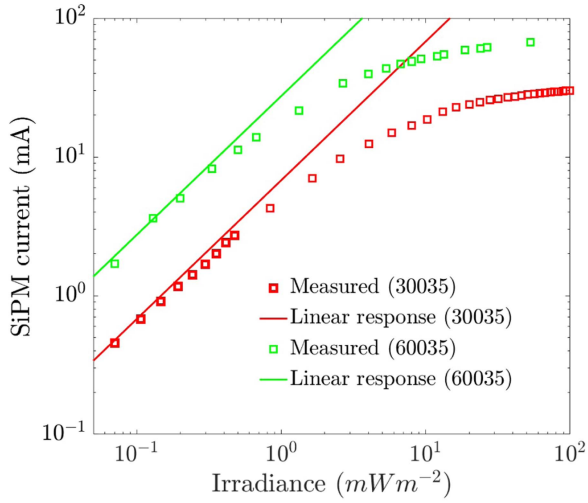

Fig. 2. The non-linear response of the 30035 and 60035 at 405 nm when biased at 28 V.

IV. Frequency Response of the Link

The second phenomenon that could impact the performance of the two SiPMs is the inter-symbol interference (ISI) caused by the fast output pulses. Table I shows that the fast output pulse widths for the 30035 and 60035 are 1.5 ns and 3 ns respectively and so the bandwidth of the 60035 is half the bandwidth of the 30035. The potential impact of the ISI caused by these output pulses means that the 3 mm by 3 mm onsemi$_{\text{TM}}$ SiPMs with narrow output pulses have recently been preferred in most VLC receivers [17], [18], [19], [21], [23].

The shape of the fast output pulses of SiPMs means that they are expected to create a single pole in the frequency domain. Furthermore, the definition of the widths of the fast output pulses and their values in the datasheet, and hence Table I, mean that these poles are expected to correspond to single pole time constants of approximately 0.7 ns and 1.4 ns.

The SiPM is expected to create a single pole in the frequency response of a VLC system. However, other parts of a system will mean that the overall frequency response is more complex than a single pole response. The frequency response of the link was therefore measured using the equipment described in the caption of Fig. 3. The results of these experiments are shown in Fig. 4. In addition, Fig. 4 shows the best fit to this measured data assuming that the responses of both systems are described as a product of two single poles. In both cases the time constants associated with the lowest frequency pole are similar to those expected from the width of the fast output pulses in the relevant datasheets. However, it appears that by slowing the recovery process the resistors on the evaluation boards containing the SiPMs have also slightly broadened the fast output pulses. In addition, the measured frequency responses of both links are consistent with a second single pole associated with time constants of 0.25 ns or 0.7 ns. Most importantly for the comparison of the two SiPMs, the different widths of the fast output pulses have a significant influence on the frequency response of the systems. In particular, the system containing the 60035 has a significantly lower bandwidth than the one containing the 30035.

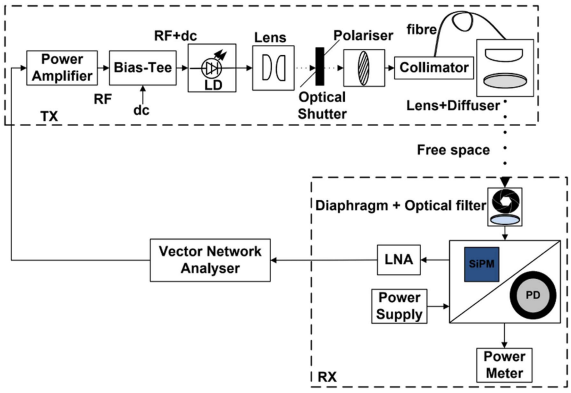

Fig. 3. Schematic diagram of the equipment used to evaluate the performance of selected J-Series SiPMs. For these measurements the signal from port 1 of a HP 8753 series vector network analyser (VNA) was amplified by a FMAM3269 (10 MHz – 6 GHz) power amplifier to produce a 1.6 Vpp output, a signal amplitude optimised for the transmission of an on-off-keying (OOK) signal. In order to bias the laser diode to an average current of 35 mA, the output signal from the power amplifier was added to a DC bias voltage of 3.3 V by a Bias-Tee (ZFBT-4R2GW+). The combined signal was then applied to a L405P20 laser diode with an output wavelength of 405 nm [23]. The light from the laser diode was then coupled to the fibre optic cable (M74L01) using two lenses (ACL25416U-A and LA1805) and a fibre collimator (F240FC). A 25 mm wire-grid polariser (34-254) from Edmund Optics was also placed between the fibre collimator and lenses. This was used to vary the light coupled to the fibre optics and hence the irradiance at the receiver. At the other end of the fibre a collimator, a lens, and an optical diffuser (DG10-220-MD) were used to create a uniformly illuminated area in which the receiver was placed. The receiver consisted of a SiPM on a SMA evaluation board, enclosed in a box. The only optical component used in the receiver was a Thorlabs FB405-10 optical bandpass filter (central wavelength 405 nm and a FWHM of 10 nm), which reduced the amount of ambient white light reaching the SiPM. A 28 V bias voltage was applied to the SiPM, so that all the microcells are biased above their breakdown voltage, and its fast output was connected to a ZX6043-S+ 4 GHz low-noise amplifier whose output was connected to port 2 of VNA.

V. Experimental Results With Equalisation

To compare the performances of receivers containing the 30035 and 60035, port 1 of the VNA was replaced by a 10 GHz Tektronix Arbitrary Waveform Generator (AWG), which was used to generate a pseudorandom binary sequence (PRBS) OOK signal. Since this signal was amplified by an amplifier (FMAM3269) that is ineffective at frequencies below 10 MHz 8b10b coding was used. On the receiver side, port 2 of the VNA was replaced by a Keysight MSOV334A oscilloscope (33 GHz, 80 GS/s) which captured the receiver output, at a rate which corresponds to 30.5 samples per bit. The captured 8b10b data was then post-processed in MATLAB. In particular, like the signal from receivers containing photodiodes or APDs, the signal was low-pass filtered. The result of this process are signals and eye diagrams, such as the one is Fig. 5, which is indistinguishable for the signals and eye diagrams obtained from receivers containing a photodiode or APD. In some experiments decision feedback equalization (DFE) was applied to this filtered signal. Finally, in all cases, the BER was calculated.

The results in Fig. 6 before DFE is applied shows the impact of the ISI arising from the finite width of the fast output pulses. In particular, the data for both SiPMs (the crosses in Fig. 6) shows a rapid increase in the required irradiance from the transmitter

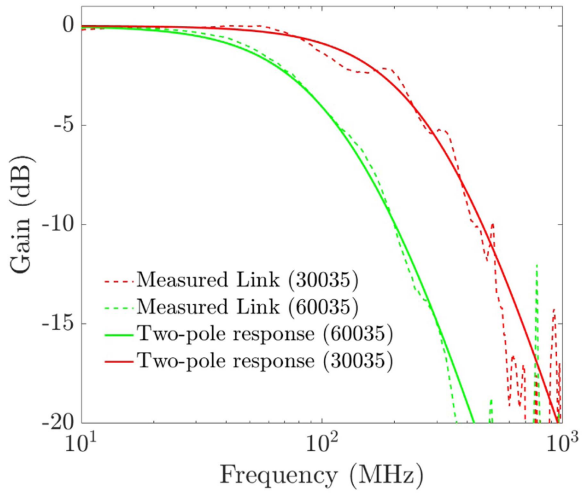

Fig. 4. The measured frequency response of the links formed with the two SiPMs. The fit to the 30035 data is a combination of two single poles with characteristic times of 0.8 ns and 0.25 ns. The fit to the 60035 data is a combination of 1.6 ns and 0.7 ns.

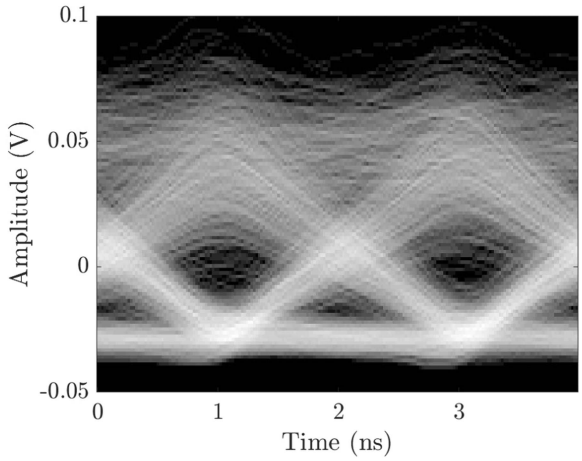

Fig. 5. The eye diagram obtained when 500 Mbps are transmitted and the output from a receiver containing a J30035 has been low pass filtered in MATLAB.

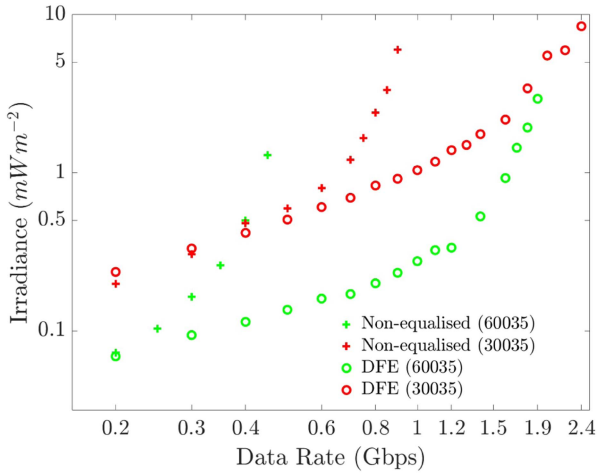

Fig. 6. The average irradiances required to transmit various OOK data rates to the two SiPMs when they are operating in the dark.

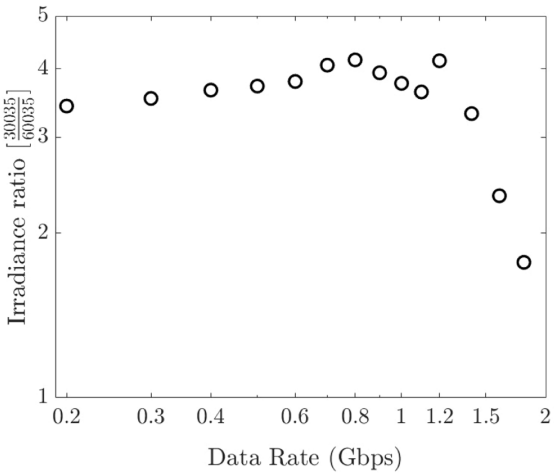

Fig. 7. The ratio of irradiances required by the 30035 and 60035 in the dark when the DFE is employed.

at the receiver once the bit time is approximately three times the characteristic time of the lowest frequency pole created by the SiPMs output pulses.

The impact of this ISI caused by the SiPMs on higher data rates can be reduced by equalizing the received signal using the DFE algorithm in MATLAB. At each data rate the recursive least squares (RLS) algorithm option was used to optimize the number of feedforward and feedback taps required to perform DFE. The equalized signal was then used to calculate the BER. A comparison of results in Fig. 6 obtained with the 30035 with equalization (red circles) to without equalization (red crosses) clearly shows that at data rates higher than 0.5 Gbps the 30035 requires a lower irradiance to achieve the same BER after equalization. Similarly, a significant reduction in the required average irradiance has been observed in the case of the 60035. However, in this case the wider output pulses of the 60035 means that equalization is beneficial for all data rates above 0.25 Gbps.

For the 30035 the irradiance needed to achieve the target BER increases rapidly for irradiances higher than approximately 2.5 mWm^{-2}. A comparison of this value with the non-linear response of the SiPM in Fig. 2 shows that this change in behavior arises from the non-linear response of the 30035. However, the irradiance at which the slope of the 60035 data in Fig. 6 changes abruptly, approximately 0.3 mWm^{-2}, is too small for this to be caused by the SiPMs non-linearity. Since it occurs at a data rate of 1.2 Gbps it may be caused by unobservable pole or poles, with a characteristic time of approximately 0.27 ns (corresponding to a 3 dB frequency of 590 MHz), in the frequency response of the link containing the 60035. Alternatively, it may be the power penalty needed to support DFE once the bit time becomes significantly shorter than the output pulse width [25].

Fig. 7 shows the ratio of the irradiances needed to transmit different OOK data rates to the links containing the 30035 and 60035 in the dark when DFE is employed. As the data rate increased the number of detected photons per bit when a zero is being transmitted decreases and so the advantage of using the 60035 increases. However, for these systems, the advantage of using the 60035 declines sharply for data rates higher than 1.2 Gbps. This decline in advantage is associated with the ISI caused by the width of the fast output pulses. Before this happens the results in Fig. 7 are consistent with the advantage predicted in Section II that didn't take into account ISI. A significant aspect of the results in Fig. 6 is that if the irradiance from transmitter is less than 3 mWm^{-2} the receiver containing the 60035 achieves higher data rates than the 30035.

VI. Predicting the Receivers' Performance

Until either the SiPM becomes non-linear, or the bit time is less than one third of the output pulse width, the results in Fig. 6 after equalization fall on a similar trend line as the results before equalization. The results before equalization can be predicted using Poisson statistics [17] and hence this observation suggests that it should be possible to predict the performance of these receivers for some data rates even after equalization. The experimental results have therefore been compared to predictions based upon Poisson statistics.

The average irradiance from the 405 nm transmitter required by the SiPM at a given data rate can be calculated using

$$I_{avg} = \frac{N_{Tx} \times E_{ph}}{T_b \times PDE \times A_{SiPM}} \tag{5}$$

where E_{ph} is the energy of photons, PDE is the photon detection efficiency of the SiPM, A_{SiPM} is the area of SiPM, and N_{Tx} is the average number of additional photons incident on the SiPM from the transmitter in a OOK bit time, T_b. However, (1) shows that this average number of photons per bit depends upon both the target BER and the total number of background counts per bit (N_b).

For the d.c. bias voltage used, the peak-to-peak voltage swing (1.6 V) applied to the laser diode in the transmitter means that it is not completely off when it transmits zeros. Therefore, the transmitter contributes to the number of background counts per bit time. Hence, the measured average irradiance (I_{avgm}), and the extinction ratio must be used to calculate the number of background counts per bit from the transmitter (N_{bTx})

$$N_{bTx} = \frac{2 \times I_{avgm} \times PDE \times A_{SiPM} \times T_b}{(1 + R_e)\, E_{ph}} \tag{6}$$

where the term $2 \times \frac{I_{avgm}}{1+R_e}$ corresponds to the irradiance (I_0) when a zero is received. Similarly, the irradiance (I_1) corresponds to irradiance when a one is received, and R_e is the extinction ratio $\frac{I1}{I0}$. To determine R_e the polarizer was set to the position it is in when 0.2 Gbps are transmitted successfully to the 30035. Then the irradiance at the receiver was measured using a Newport 818-SL optical power detector with the minimum voltage, 2.5 V, and the maximum voltage, 4.1 V, applied to the laser diode. The ratio of these two measurements showed that the extinction ratio was 15.

Fig. 8 shows that for the 30035 the average irradiance (red solid-line) predicted using the measured extinction ratio and Poisson statistics matches the results (red circles) achieved with DFE up to 1.4 Gbps. The results then deviate from the prediction at higher data rates. However, as discussed in Section V, this

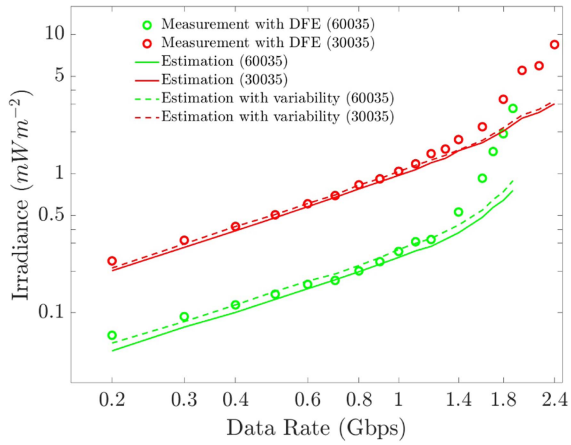

Fig. 8. The measured and estimated average irradiance required to transmit various OOK data rates to the 30035 and the 60035 in the dark.

TABLE II
MEAN AND STANDARD DEVIATION OF INTEGRAL VALUE OF PRIMARY DARK PULSES

Mean (μ)	30035	4.84×10^{-3}
	60035	1×10^{-2}
Standard Deviation (σ)	30035	7.9×10^{-4}
	60035	4×10^{-3}

deviation occurs as result of the non-linearity of the 30035 which is not taken into account by the prediction.

A similar behaviour can be observed in the case of the 60035. However, the results (green circles) in Fig. 8 show a deviation from the estimated average irradiance (green solid line) at data rates above 1.2 Gbps. However, even at the lowest data rates the prediction of the performance of the 60035 isn't as good as the prediction for the 30035. Furthermore, since equalization isn't needed for the lowest two data rates any difference between the predicted and the measured irradiances can't be caused by ISI.

After considering possible explanations for the difference between the predicted and the measured results for the 60035 the variability of fast output pulses was investigated. When the SiPM is used as a receiver its fast output signal is captured and low-pass filtered in the same way as the analog signal from a conventional receiver. Consequently, the important characteristic of the captured output pulses is their integral.

Fig. 9 shows the distributions of the integrals over a time of twice the fast output pulse width of approximately 500 single fast output pulses from the 30035 and the 60035. The means and standard deviations of these integrals, listed in Table II, show that for the 30035 the standard deviation (σ) of the distribution is 16% of the mean value. However, for the 60035 the standard deviation of the distribution is 40% of the mean value. The fast output pulses from the 60035 are therefore significantly more variable when compared to their mean than the fast output pulses from the 30035.

The variability of output pulses is an additional noise source which can be taken into account by increasing the dominant noise source, which is the number of background counts per bit.

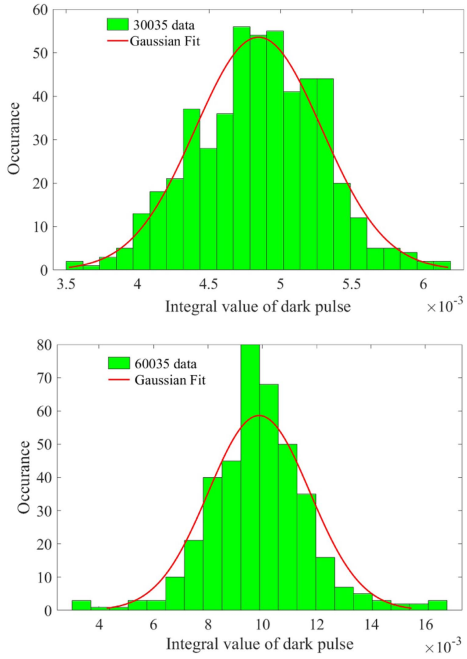

Fig. 9. Distribution of integral value of dark pulses captured from the fast output of the 30035 (top) and the 60035 (bottom). Solid line shows Gaussian fit to the distribution.

In particular, for the 30035 the number of background photons per bit have been multiplied by 1.16, whilst for the 60035 the multiplier was 1.4. These increased values were then substituted in (1). The value of n_{Tx} and the corresponding average irradiance required from the 405 nm transmitter was estimated using (5).

The red and green dotted lines in Fig. 8 are the revised versions of the average irradiance estimated with variations in output pulses taken into account. In the case of the 30035, only a slight difference is observed between the revised prediction (red dotted line) and previous prediction (red solid line). The variability of the fast output pulses from the 30035 therefore has little impact on its performance. In contract, the revised prediction for the 60035 (green dotted line), is noticeable closer to the measured data than the previous prediction (green solid line). This shows that the variability of the fast output pulses can have a noticeable impact on the receiver performance. The variability of output pulses should therefore be taken into consideration when selecting which SiPMs to use in receivers or when designing a new SiPM specifically for VLC systems. More importantly, until the SiPM becomes non-linear or the OOK bit time is less than one third of the output pulse width the performance of a SiPM containing receiver can be predicted using Poisson statistics.

VII. SELECTING A SIPM FOR A NEAR INFRARED LINK

Near infra-red wavelengths, for example 850 nm, are of interest for a variety of reasons, including the availability of high bandwidth transmitters and the higher eye safe irradiances. An additional advantage when using a receiver containing a SiPM is that when compared to systems using 405 nm there are more than twice the number of photons per Watt. Previously, the R series of SiPMs, which had been designed to have a maximum

TABLE III
ONSEMI™ RB-SERIES SIPMS

Parameter	SiPM		
	10010	10020	10035
Area [mm^2]	1	1	1
Microcell Pitch [μm]	10	20	35
Number of Microcells	4296	1590	620
Recovery Time [ns]	12	21	73
Maximum Count Rate (Gcps)	163	34	4
PDE [@850 nm]	0.07	0.12	0.17

PDE around 600 nm rather than 420 nm, have been suggested for use at 850 nm [26].

The results for both the 30035 and 60035 show that after DFE is applied Poisson statistics can be used to predict the performance of a link until the SiPM starts to saturate or the OOK bit time is less than one third of the output pulse width. If these conditions are satisfied the achievable BER is determined by the additional number of detected photons per bit time when a 1 is received. In addition, for free-space links the divergence of light from the transmitter means that it is the irradiance at the receiver that is important [22]. Consequently, an important consideration when selecting a SiPM for incorporation in a receiver for a free space VLC system is the product of the PDE at the transmitter's wavelength and the area of the SiPM.

The R series has been replaced by the RB series of SiPMs. However, as shown in Table III, like the R series, the SiPMs in the RB series are all 1 mm^2 and have PDEs at 850 nm ranging from 7% to 17%. In contrast, although its maximum PDE occurs at 420 nm the PDE of the 60035 at 850 nm is approximately 3% [27]. The larger area of the 60035 therefore more than compensates for this lower PDE at 850 nm. Consequently, for operation at data rates up to at least 1 Gbps the 60035 is a better choice for use in a receiver of 850 nm than any SiPM in the RB series. However, if a 6 mm by 6 mm RB series SiPM with a 35 μm microcell was manufactured the PDEs suggest that, as long as it remains in its linear region of operation, it would be expected to need less than one fifth of the irradiance required by the J series 60035 to support the same BER and data rate.

VIII. CONCLUSION

Poisson statistics suggest that increasing the area of SiPMs in VLC receivers will reduce the irradiance needed to achieve the same BER and data rate. In particular, if the number of detected photons per bit when a zero is transmitted is negligible increasing the area by a factor M will reduce the required irradiance by a factor of M. However, when more than 10 photons are detected in each bit time when a zero is transmitted Gaussian statistics apply and increasing the area of the SiPM by a factor M will reduce the irradiance by a factor of M$^{1/2}$. The benefits of using a larger SiPM will therefore be increased if the SiPM is protected from ambient light and the transmitter has a high extinction ratio.

However, predictions based upon statistics alone don't take into account either the non-linear response of the SiPMs or the width of their output pulses. Two SiPMs with different areas and output pulse widths have been characterized and incorporated into VLC receivers. Results show that, until the SiPM becomes non-linear or another part of the VLC link impacts its frequency response or the OOK bit time is less than a third of the width of the output pulses, the results after DFE fall on the trend line of the results at low data rates. Consequently, under these conditions, the performance of a VLC link containing a SiPM receiver can be predicted using Poisson statistics alone. Hence, when both the SiPMs have a linear response the 60035 supports the same BER and data rate as the 30035 with between one quarter and one half of the irradiance needed by the 30035.

The overall conclusion is that, unless the OOK bit time is shorter than one third of the output pulse width, the bandwidth of a SiPM should not be a high priority when selecting a SiPM for incorporation in a VLC receiver. Furthermore, for these data rates, until their non-linearity or the frequency response of another part of the VLC link become important, Poisson statistics can be used to predict the performance of VLC links containing SiPMs in different scenarios.

A combination of Poisson statistics and the importance of irradiance in free space links means that an important consideration when selecting a SiPM for incorporation in a VLC receiver is the product of the PDE at the transmitter's wavelength and the area of the SiPM. At the moment this means that the J series 60035 is expected to be a better choice than any of the RB series SiPMs for systems working in the near-infrared.

Further work is required to determine the selection criteria that should be used when the OOK bit time is less than one third of the output pulse width. The results presented in this paper show that it is difficult to separate the effects of the SiPM non-linearity and output pulse widths experimentally. The best approach to conclusively separating these two effects is therefore to use a numerical simulation so that each characteristic of the simulated SiPM can be varied independently.

REFERENCES

[1] F. Zafar, M. Bakaul, and R. Parthiban, "Laser-diode-based visible light communication: Toward gigabit class communication," *IEEE Commun. Mag.*, vol. 55, no. 2, pp. 144–151, Feb. 2017, doi: 10.1109/MCOM.2017.1500672CM.

[2] D. O'Brien, S. Rajbhandari, and H. Chun, "Transmitter and receiver technologies for optical wireless," *Philos. Trans. Roy. Soc. A: Math., Phys. Eng. Sci.*, vol. 378, no. 2169, 2020, Art. no. 20190182, doi: 10.1098/rsta.2019.0182.

[3] A. Eisele and R. Henderson, "185 MHz count rate, 139 dB dynamic range single-photon avalanche diode with active quenching circuit in 130 nm CMOS technology," in *Proc. Int. Image Sensor Workshop*, 2011, pp. 6–8.

[4] E. Fisher, I. Underwood, and R. Henderson, "A reconfigurable 14-bit 60 GPhoton/s single-photon receiver for visible light communications," in *Proc. Eur. Solid-State Circuits Conf.*, 2012, pp. 85–88, doi: 10.1109/ESSCIRC.2012.6341262.

[5] D. Chitnis and S. Collins, "A SPAD-based photon detecting system for optical communications," *J. Lightw. Technol.*, vol. 32, no. 10, pp. 2028–2034, May 2014, doi: 10.1109/JLT.2014.2316972.

[6] O. Almer et al., "A SPAD-based visible light communications receiver employing higher order modulation," in *Proc. IEEE Glob. Commun. Conf.*, 2015, pp. 1–6, doi: 10.1109/GLOCOM.2014.7417269.

[7] Y. Li, M. Safari, R. Henderson, and H. Haas, "Optical OFDM with single-photon avalanche diode," *IEEE Photon. Technol. Lett.*, vol. 27, no. 9, pp. 943–946, May 2015, doi: 10.1109/LPT.2015.2402151.

[8] T. Jukić, B. Steindl, and H. Zimmermann, "400 µm diameter APD OEIC in 0.35 µm BiCMOS," *IEEE Photon. Technol. Lett.*, vol. 28, no. 18, pp. 2004–2007, Sep. 2016, doi: 10.1109/LPT.2016.2578979.

[9] J. Zhang, L. - H. Si-Ma, B. - Q. Wang, J. - K. Zhang, and Y. - Y. Zhang, "Low-complexity receivers and energy-efficient constellations for SPAD VLC systems," *IEEE Photon. Technol. Lett.*, vol. 28, no. 17, pp. 1799–1802, Sep. 2016, doi: 10.1109/LPT.2016.2572300.

[10] T. Mao, Z. Wang, and Q. Wang, "Receiver design for SPAD-based VLC systems under Poisson–Gaussian mixed noise model," *Opt. Exp.*, vol. 25, no. 2, pp. 799–809, Jan. 2017, doi: 10.1364/oe.25.000799.

[11] M. Khalighi, T. Hamza, S. Bourennane, P. Léon, and J. Opderbecke, "Underwater wireless optical communications using silicon photomultipliers," *IEEE Photon. J.*, vol. 9, no. 4, Aug. 2017, Art. no. 7905310, doi: 10.1109/JPHOT.2017.2726565.

[12] C. Wang, H. - Y. Yu, Y. - J. Zhu, T. Wang, and Y. - W. Ji, "Multiple-symbol detection for practical SPAD-based VLC system with experimental proof," in *Proc. IEEE Globecom Workshops*, 2017, pp. 1–6, doi: 10.1109/GLOCOMW.2017.8269144.

[13] C. Wang, H. - Y. Yu, Y. - J. Zhu, T. Wang, and Y. - W. Ji, "Multi-LED parallel transmission for long distance underwater VLC system with one SPAD receiver," *Opt. Commun.*, vol. 410, pp. 889–895, Mar. 2018, doi: 10.1016/j.optcom.2017.11.069.

[14] Y. - D. Zang, J. Zhang, and L. - H. Si-Ma, "Anscombe root DCO-OFDM for SPAD-based visible light communication," *IEEE Photon. J.*, vol. 10, no. 2, Apr. 2018, Art. no. 7902509, doi: 10.1109/JPHOT.2017.2785798.

[15] L. Zhang et al., "A comparison of APD- and SPAD-based receivers for visible light communications," *J. Lightw. Technol.*, vol. 36, no. 12, pp. 2435–2442, Jun. 2018, doi: 10.1109/JLT.2018.2811180.

[16] J. Kosman et al., "A 500 Mb/s −46.1 dBm CMOS SPAD receiver for laser diode visible-light communications," in *Proc. IEEE Int. Solid- State Circuits Conf.*, 2019, pp. 468–470, doi: 10.1109/ISSCC.2019.8662427.

[17] Z. Ahmed, L. Zhang, G. Faulkner, D. O'Brien, and S. Collins, "A shot-noise limited 420 Mbps visible light communication system using commerical off-the-shelf silicon photomultiplier (SiPM)," in *Proc. IEEE Int. Conf. Commun. Workshops*, 2019, pp. 1–5, doi: 10.1109/ICCW.2019.8757030.

[18] Z. Ahmed, R. Singh, W. Ali, G. Faulkner, D. O'Brien, and S. Collins, "A SiPM-based VLC receiver for Gigabit communication using OOK modulation," *IEEE Photon. Technol. Lett.*, vol. 32, no. 6, pp. 317–320, Mar. 2020.

[19] L. Zhang et al., "Over 10 attenuation length gigabits per second underwater wireless optical communication using a silicon photomultiplier (SiPM) based receiver," *Opt. Exp.*, vol. 28, no. 17, pp. 24968–24980, Aug. 2020, doi: 10.1364/oe.397942.

[20] M. A. Khalighi, H. Akhouayri, and S. Hranilovic, "Silicon-photomultiplier-based underwater wireless optical communication using pulse-amplitude modulation," *IEEE J. Ocean. Eng.*, vol. 45, no. 4, pp. 1611–1621, Oct. 2020, doi: 10.1109/JOE.2019.2923501.

[21] W. Matthews, Z. Ahmed, W. Ali, and S. Collins, "A 3.45 gigabits/s SiPM-based OOK VLC receiver," *IEEE Photon. Technol. Lett.*, vol. 33, no. 10, pp. 487–490, May 2021, doi: 10.1109/LPT.2021.3069802.

[22] W. Ali, G. Faulkner, Z. Ahmed, W. Matthews, and S. Collins, "Gigabit transmission between an eye-safe transmitter and wide field-of-view SIPM receiver," *IEEE Access*, vol. 9, pp. 154225–154236, 2021, doi: 10.1109/ACCESS.2021.3116704.

[23] S. Huang, C. Chen, R. Bian, H. Haas, and M. Safari, "5 Gbps optical wireless communication using commercial SPAD array receivers," *Opt. Lett.*, vol. 47, pp. 2294–2297, 2022, doi: 10.1364/OL.454994.

[24] Onsemi.com, *J-Series SiPM Sensors Datasheet*, 2020. Accessed: Jun. 20, 2022. [Online]. Available: https://www.onsemi.com/pub/Collateral/MICROJ-SERIES-D.PDF

[25] S. Randel, F. Breyer, S. C. J. Lee, and J. W. Walewski, "Advanced modulation schemes for short-range optical communications," *IEEE J. Sel. Topics Quantum Electron.*, vol. 16, no. 5, pp. 1280–1289, Sep./Oct. 2010, doi: 10.1109/JSTQE.2010.2040808.

[26] S. Huang and M. Safari, "Hybrid SPAD/PD receiver for reliable free-space optical communication," *IEEE Open J. Commun. Soc.*, vol. 1, pp. 1364–1373, 2020, doi: 10.1109/OJCOMS.2020.3023009.

[27] RB-SERIES SIPM: Silicon Photomultipliers, NIR-Enhanced', Aug. 2021. Accessed: Sep. 15, 2022. [Online]. Available: https://www.onsemi.com/products/sensors/photodetectors-sipm-spad/silicon-photomultipliers-sipm/rb-series-sipm